

Force-induced desorption of self-avoiding walks on Sierpinski gasket fractals

I. Vidanović¹, S. Arsenijević², and S. Elezović-Hadžić^{3,a}

¹ Scientific Computing Laboratory, Institute of Physics Belgrade, University of Belgrade, Pregrevica 118, 11080 Belgrade, Serbia

² Institute of Condensed Matter Physics, EPFL, 1015 Lausanne, Switzerland

³ University of Belgrade, Faculty of Physics, P.O. Box 44, 11001 Belgrade, Serbia

Received 22 November 2010 / Received in final form 5 March 2011

Published online 28 March 2011 – © EDP Sciences, Società Italiana di Fisica, Springer-Verlag 2011

Abstract. In this work we investigate force-induced desorption of linear polymers in good solvents in non-homogeneous environment, by applying the model of self-avoiding walk on two- and three-dimensional fractal lattices, obtained as generalization of the Sierpinski gasket fractal. For each of these lattices one of its boundaries represents an adsorbing wall, whereas along one of the fractal edges, not lying in the adsorbing wall, an external force acts on the self-avoiding walk. The hierarchical nature of the lattices under study enables an exact real-space renormalization group treatment, which yields the phase diagram of polymer critical behavior. We show that for this model there is no low-temperature reentrance in the cases of two-dimensional lattices, whereas in all studied three-dimensional cases the force-temperature dependence is reentrant. We also find that in all cases the force-induced desorption transition is of first order.

1 Introduction

Adsorption of polymer chains on surfaces is a phenomenon of wide occurrence in many industrial and daily processes and it also plays an important role in functioning of biological systems. Recent progress in atomic force microscopy and development of optical and magnetic tweezer techniques made it possible to micromanipulate a single polymer chain [1]. Using these experimental methods one can measure the force needed to detach a chain from an adsorbing surface and monitor the mechanism of some force-driven phase transitions at the level of a single molecule. Such experiments initiated a number of theoretical studies with the aim to obtain a deeper insight into the thermodynamics of force-induced desorption of a polymer. These studies pursue an extensive theoretical work on the polymer adsorption problem performed in the last decades [2–4], and include approaches based on mean-field type approximations, scaling arguments, Monte Carlo simulations and exactly solvable models [5–19].

A common physical situation treated theoretically in the context of force-induced polymer desorption is the following: a linear polymer molecule is tethered at one end to an impenetrable surface, at which the polymer can adsorb, and to the other end of the polymer a force is applied. When the polymer is pulled away from the surface, one expects a critical value of the force $f_c(T)$ (which depends on the temperature T), such that for $f < f_c(T)$ the

polymer is adsorbed, while for $f > f_c(T)$ it is desorbed. Thus, the curve $f_c(T)$ can be regarded as a boundary that separates the desorbed phase from the adsorbed phase in the (T, f) plane. This phase transition was usually studied within the models in which the polymer is in a homogeneous environment, whereas in real situations one can expect different kinds of obstacles, which make some parts of the environment not accessible to the polymer. For instance, in biological systems the adsorption of polymer molecules on membranes occurs in cells which are crowded with various biomolecules, that may occupy a large fraction of the cell volume. However, exact treatment of such heterogeneities is difficult, therefore in this paper we use a simplified approach in which the polymer is modeled by a self-avoiding walk (SAW) on deterministic fractal lattices. Such models were often used and proved to be very useful in analytical investigation of various aspects of polymer behavior in non-homogeneous media (see [20] for a recent review). Here, by applying an exact real-space renormalization group (RG) method, in Section 2 we consider SAW on the Sierpinski gasket (SG) fractal, one of its boundary edges representing an adsorbing wall, whereas an external force, directed along the other fractal edge, is pulling the SAW from the wall. We show that unbinding occurs at some critical value of the force and obtain the corresponding phase diagram in the force-temperature plane. In Section 3 we generalize this approach to the Given-Mandelbrot (GM) fractal family, explicitly obtain phase diagrams for several GM fractals, show that for all of them

^a e-mail: suki@ff.bg.ac.rs

the unbinding phase transition is of first order, and that critical force is monotonically decreasing function of temperature. Case of the three-dimensional generalization of the SG fractal is considered in Section 4, where it is found that corresponding critical force diagram is reentrant, i.e. in the low temperatures region, the critical force increases with the temperature, whereas in the high temperature region it decreases, thus having a maximum for some intermediate temperature. All obtained results are summarized and compared with related previous results, and possible extensions of the presented investigation are outlined in the last section. Finally, some technical details are given in the Appendixes.

2 Force-induced desorption in the case of the two-dimensional Sierpinski gasket lattice

In order to investigate the problem of the force-induced desorption of a linear polymer, in this Section we model the polymer by a self-avoiding walk (SAW) on two-dimensional Sierpinski gasket (2d SG) fractal. This fractal is a well known lattice, which can be constructed recursively, starting with the generator, comprised of three upward-oriented unit equilateral triangles. The subsequent fractal stages are constructed self-similarly, by replacing each of the unit triangles of the initial generator by a new generator (Fig. 1). To obtain the k th-stage ($-$ order) fractal lattice, this process of construction has to be repeated $(k - 1)$ times, and the complete 2d SG fractal is obtained in the limit $k \rightarrow \infty$. Pure adsorption of SAW on 2d SG was analyzed in [21], where interaction between polymer and surface (i.e. one boundary of the lattice) was described by two Boltzmann factors: $w = \exp(-\varepsilon_w/k_B T) > 1$ and $t = \exp(-\varepsilon_t/k_B T) < 1$. The factor w corresponds to an attractive interaction between the wall and the polymer chain segments lying in it, implying that $\varepsilon_w < 0$ is the energy of a monomer at the boundary, whereas the factor t takes into account repulsive interaction between the surface and the chain segments in the first neighborhood of the wall, i.e. $\varepsilon_t > 0$ is the energy of a monomer in the layer adjacent to the surface. To a single step of the SAW a weight x (fugacity) is assigned, so that to each N -step walk, having M steps along the wall, and R steps in the layer adjacent to the wall, the weight $x^N w^M t^R$ is associated. Due to the finite ramification of the SG lattice, the statistics of this polymer model can be studied exactly, introducing three restricted partition functions A , A_w , and A_t , which are defined as weighted sums over the SAW paths within a finite stage k of the construction of the fractal:

$$A^{(k)}(x) = \sum_N \mathcal{A}^{(k)}(N) x^N, \quad (1)$$

$$A_w^{(k)}(x, w, t) = \sum_{N, M, R} \mathcal{A}_w^{(k)}(N, M, R) x^N w^M t^R, \quad (2)$$

$$A_t^{(k)}(x, w, t) = \sum_{N, M, R} \mathcal{A}_t^{(k)}(N, M, R) x^N w^M t^R. \quad (3)$$

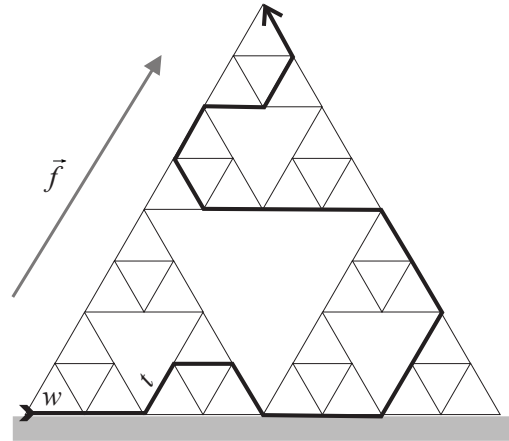


Fig. 1. An example of self-avoiding walk traversing the structure obtained after the third step of the recursive construction of the two-dimensional Sierpinski gasket fractal. Horizontal boundary of the lattice represents the attractive wall, whereas the force \vec{f} is directed along the second boundary. Length of the SAW is $N = 19$, number of steps at the wall is $M = 4$, number of steps at the layer adjacent to the wall is $R = 3$, and the projection of the walk along the direction of \vec{f} is $L = 8$, therefore the weight of this SAW is $x^{19} w^4 t^3 y^8$.

In particular, $\mathcal{A}^{(k)}(N)$ is the number of N -step SAWs, traversing the k th order SG which is completely in the bulk, whereas $\mathcal{A}_w^{(k)}(N, M, R)$ and $\mathcal{A}_t^{(k)}(N, M, R)$ are the numbers of N -step SAWs that traverse the k th order SG at the boundary (as depicted in Fig. 2a), and have M steps along the adsorbing boundary and R steps at the layer adjacent to it. Function A satisfies the recursion relation

$$A^{(k+1)} = (A^{(k)})^2 + (A^{(k)})^3, \quad (4)$$

and can be interpreted as a renormalization group (RG) equation [22,23]. Its only nontrivial fixed point $A^* = (\sqrt{5} - 1)/2$ is reached starting with the initial value $A^{(0)} = x^1$, for the critical value of fugacity equal to $x = x^* = A^*$. This fixed point corresponds to the state in which SAW is in the form of the swollen isotropic coil in the bulk, with its average end-to-end distance $\langle R \rangle$ scaling as $\langle R \rangle \sim \langle N \rangle^\nu$, where $\langle N \rangle$ is the average SAW length. Within the RG framework the critical exponent ν can be calculated as $\nu = \ln 2 / \ln \lambda_\nu = 0.7986$, where $\lambda_\nu = 2A^* + 3A^{*2}$ is the eigenvalue of the bulk equation (4), linearized in the vicinity of the fixed point A^* . As elaborated in [21], numerical analysis of the RG equations

$$\begin{aligned} A_w^{(k+1)} &= (A_w^{(k)})^2 + A^{(k)}(A_t^{(k)})^2, \\ A_t^{(k+1)} &= A^{(k)} A_t^{(k)} (1 + A_w^{(k)}), \end{aligned} \quad (5)$$

satisfied by the surface-functions $A_w^{(k)}$ and $A_t^{(k)}$, accompanied by the recursion relation (4) for the bulk function $A^{(k)}$, reveals that for each value of $0 < t < 1$, there exists a critical value of $w = w^*(t)$, such that:

¹ Such initial condition correspond to the SAW model in which unit triangle can be traversed only along one of its three edges, which does not alter the critical behavior of the model.

- for $w < w^*(t)$ and $x = x^*$, RG parameters flow towards the fixed point $(A, A_w, A_t)^* = (A^*, 0, 0)$, i.e. SAW is in the desorbed phase;
- when $w > w^*(t)$ and $x = x_c(w, t) < x^*$, the fixed point $(A, A_w, A_t)^* = (0, 1, 0)$ is reached, so that SAW is completely adsorbed at the boundary;
- precisely at the critical value $w = w^*(t)$, and for $x = x^*$, the symmetrical fixed point

$$(A, A_w, A_t)^* = (A^*, A^*, A^*) \quad (6)$$

is approached, corresponding to the transition from adsorbed to desorbed phase. At this point average number $\langle M \rangle$ of SAW steps that lie in the surface, scales with the SAW average length $\langle N \rangle$ according to the relation $\langle M \rangle \sim \langle N \rangle^\phi$. So-called crossover exponent ϕ is equal to $\phi = \ln \lambda_\phi / \ln \lambda_\nu = 0.5915$, where λ_ϕ is the second largest eigenvalue of the RG equations (4)–(5), linearized in the vicinity of the fixed point (6).

2.1 Introducing the force

To introduce the external force f into the described polymer model, we add the third Boltzmann factor $y = \exp(f/k_B T)$, so that the weight of N -step SAW is $x^N w^M t^R y^L$ (Fig. 1), where L is the length of SAW's projection along the direction of \mathbf{f} , measured in elementary triangle edges, while M and R have the same meaning as in the pure adsorption case. Here we assume that the force \mathbf{f} is parallel to one of the two lattice boundaries, which do not coincide with the adsorbing boundary. The statistics of this extended model can be studied exactly, introducing 10 restricted partition functions: $F_i^{(k)}(x, y)$, $i = 1, 4$, and $G_i^{(k)}(x, y, w, t)$, $i = 1, 6$ (see Fig. 2b). These functions are defined as weighted sums over the SAW paths within a finite stage k of the fractal construction:

$$F_i^{(k)}(x, y) = \sum_{N, L} \mathcal{F}_i^{(k)}(N, L) x^N y^L, \quad (7)$$

$$G_i^{(k)}(x, y, w, t) = \sum_{N, M, R, L} \mathcal{G}_i^{(k)}(N, M, R, L) x^N w^M t^R y^L. \quad (8)$$

Here, numbers $\mathcal{F}_i^{(k)}$ are generalization of the number $\mathcal{A}^{(k)}$, when projection of the SAW on the force direction is taken into account. The subscript i enumerates different possibilities for values of the angle between the force direction and the vector determined by entering and exiting point of the SAW traversing the k th order SG, as it is sketched in Figure 2b. In a similar way, $\mathcal{G}_i^{(k)}$ are generalization of the numbers $\mathcal{A}_w^{(k)}$ and $\mathcal{A}_t^{(k)}$, i.e.

$\mathcal{G}_i^{(k)}(N, M, R, L)$ are numbers of N -step SAWs, traversing the k th order SG lying on the surface, whose projection along \mathbf{f} is equal to L , and which have M steps in the surface and R steps in the layer adjacent to it. From the definition of the force-functions $F_i^{(k)}$ it directly follows

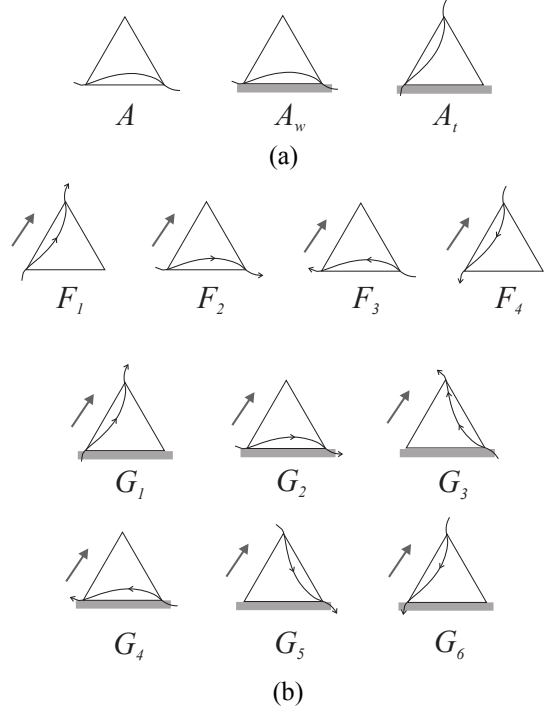


Fig. 2. (a) To analyze the adsorption of SAWs on 2d SG fractal structures (represented by triangles) one needs three restricted partition functions, corresponding to configurations A , A_w and A_t [21]. (b) When force acts on polymer chain (full curved lines), one has to consider the orientation of SAWs, which brings about 10 different configurations: F_i , $i = 1, 4$ and G_i , $i = 1, 6$.

that they can be expressed as

$$\begin{aligned} F_1^{(k)} &= y^{2^k} A^{(k)}, & F_2^{(k)} &= y^{2^{k-1}} A^{(k)}, \\ F_3^{(k)} &= y^{-2^{k-1}} A^{(k)}, & F_4^{(k)} &= y^{-2^k} A^{(k)}, \end{aligned} \quad (9)$$

whereas the force-surface-functions $G_i^{(k)}$ are equal to

$$\begin{aligned} G_1^{(k)} &= y^{2^k} A_t^{(k)}, & G_2^{(k)} &= y^{2^{k-1}} A_w^{(k)}, \\ G_3^{(k)} &= y^{2^{k-1}} A_t^{(k)}, & G_4^{(k)} &= y^{-2^{k-1}} A_w^{(k)}, \\ G_5^{(k)} &= y^{-2^{k-1}} A_t^{(k)}, & G_6^{(k)} &= y^{-2^k} A_w^{(k)}. \end{aligned} \quad (10)$$

Detailed numerical analysis of the behavior of the functions $F_i^{(k)}$ and $G_i^{(k)}$ (see Appendix A), for large set of possible x , y , w and t values, shows that:

1. For every $y > 1$ and $0 < t < 1$ exist values of the fugacity x and interaction parameter w : $x = x_c(y)$ (Fig. 3) and $w = w_c(y, t)$ (Fig. 4) such that starting with the initial values

$$A^{(0)} = x, \quad A_w^{(0)} = xw, \quad A_t^{(0)} = xt, \quad (11)$$

and iterating relations (4) and (5), together with (9) and (10), the fixed point

$$\begin{aligned} (F_1, F_2, F_3, F_4)^* &= (1, 0, 0, 0), \\ (G_1, G_2, G_3, G_4, G_5, G_6)^* &= (G_1^*, 1, 0, 0, 0, 0) \end{aligned} \quad (12)$$

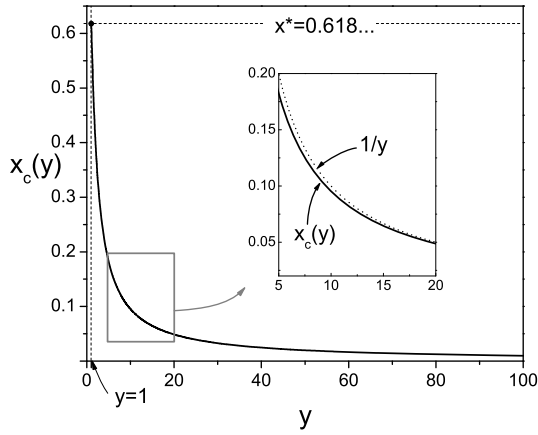


Fig. 3. Critical values of the fugacity $x_c(y)$, $y > 1$, for which functions $F_i^{(k)}(x, y)$ reach the fixed point $(F_1, F_2, F_3, F_4)^* = (1, 0, 0, 0)$, corresponding to elongated self-avoiding walk in the “bulk” of the 2d Sierpinski gasket. The part corresponding to the range of y values from 5 to 20 is magnified in the inset, where dotted line represents the function $1/y$. It can be seen that already for these, relatively small values of y , the difference between $x_c(y)$ and $1/y$ is almost negligible.

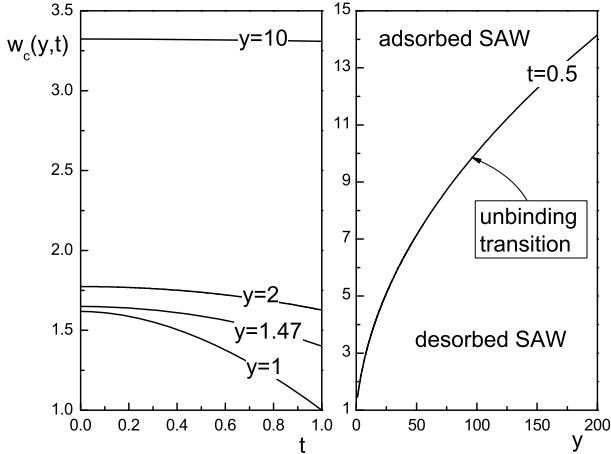


Fig. 4. Set of the critical values $w_c(y, t)$, dividing areas corresponding to the adsorbed and desorbed phase of the self-avoiding chain on the Sierpinski gasket lattice. On the left-hand side w_c is presented as a function of t for several fixed values of y , whereas the line on the right-hand side corresponds to $w_c(y, t = 0.5)$.

is reached, where value $G_1^* > 0$ depends on the particular values of t and y . The structure of this fixed point indicates that SAW is elongated ($F_1^* = 1$), but still the large number of monomers are adsorbed ($G_2^* = 1$). This situation corresponds to the coexistence between adsorbed and desorbed polymer phases.

- For $w < w_c(y, t)$, $x = x_c(y)$, $y > 1$ and $0 < t < 1$ the fixed point

$$\begin{aligned} (F_1, F_2, F_3, F_4)^* &= (1, 0, 0, 0), \\ (G_1, G_2, G_3, G_4, G_5, G_6)^* &= (G_1^*, 0, 0, 0, 0, 0) \end{aligned} \quad (13)$$

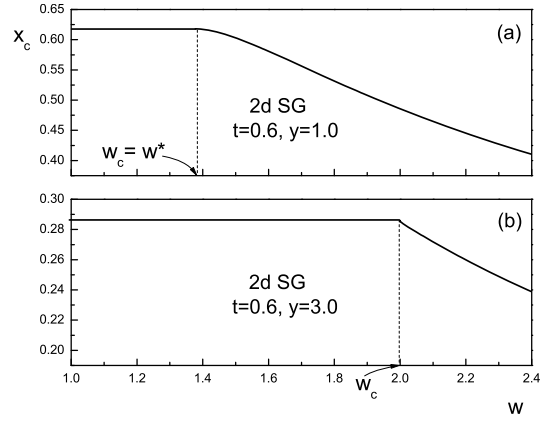


Fig. 5. Critical value of the fugacity x_c for the two-dimensional Sierpinski gasket fractal, as a function of w , for $t = 0.6$ and (a) $y = 1.0$, and (b) $y = 3.0$. In both cases the critical fugacity x_c is constant in the range $1 \leq w \leq w_c(y, t)$, and starts to decrease at the critical value w_c , which corresponds to the unbinding transition. It can be seen that the first derivative of x_c at the transition point is continuous for the pure adsorption (a), and discontinuous when the force is present (b), indicating that the acting force changes the unbinding transition order.

is approached after sufficient number of iterations k . Polymer is desorbed ($G_2^* = 0$) and elongated ($F_1^* = 1$) along the direction of the force.

- When $w > w_c(y, t)$, for any $y > 1$ and $0 < t < 1$, there exists the critical value of the fugacity $x = x_c(w, y, t) < x_c(y)$ (see Fig. 5), for which the fixed point

$$\begin{aligned} (F_1, F_2, F_3, F_4)^* &= (0, 0, 0, 0), \\ (G_1, G_2, G_3, G_4, G_5, G_6)^* &= (0, 1, 0, 0, 0, 0) \end{aligned} \quad (14)$$

is obtained. Since $G_2^* = 1$ and all the other G_i^* and F_i^* are equal to 0, in this phase SAW is completely adsorbed.

The physical meaning of these numerically established fixed points can be further confirmed by calculating the average number $\langle M \rangle^{(k)}$ of SAW steps at the attractive wall, by applying the grand canonical ensemble formalism. In particular, taking $G_1^{(k)} + G_2^{(k)}$ as a grand canonical partition function for all possible SAWs, beginning at the lower left corner of the k th order gasket (lying on the surface), and leaving it through one of the remaining two corners, one can easily obtain the following formula

$$\begin{aligned} \langle M \rangle^{(k)} &= \frac{w}{G_1^{(k)} + G_2^{(k)}} \left(\frac{\partial G_1^{(k)}}{\partial w} + \frac{\partial G_2^{(k)}}{\partial w} \right) \\ &= \frac{w}{y^{2k} A_t^{(k)} + y^{2k-1} A_w^{(k)}} \left(y^{2k} \frac{\partial A_t^{(k)}}{\partial w} + y^{2k-1} \frac{\partial A_w^{(k)}}{\partial w} \right). \end{aligned} \quad (15)$$

In a similar manner the SAW average length $\langle N \rangle^{(k)}$ can be expressed as

$$\begin{aligned} \langle N \rangle^{(k)} &= \frac{x}{G_1^{(k)} + G_2^{(k)}} \left(\frac{\partial G_1^{(k)}}{\partial x} + \frac{\partial G_2^{(k)}}{\partial x} \right) \\ &= \frac{x}{y^{2^k} A_t^{(k)} + y^{2^{k-1}} A_w^{(k)}} \left(y^{2^k} \frac{\partial A_t^{(k)}}{\partial x} + y^{2^{k-1}} \frac{\partial A_w^{(k)}}{\partial x} \right). \end{aligned} \quad (16)$$

On the other hand, from the recursion relations for the bulk and surface restricted partition functions A , A_w , and A_t (Eqs. (4) and (5)), it follows that the recursion relations for their derivatives can be expressed in matrix form as:

$$\begin{aligned} \begin{pmatrix} \frac{\partial A^{(k+1)}}{\partial x} \\ \frac{\partial A_w^{(k+1)}}{\partial x} \\ \frac{\partial A_t^{(k+1)}}{\partial x} \end{pmatrix} &= \begin{pmatrix} \frac{\partial A^{(k+1)}}{\partial A^{(k)}} & 0 & 0 \\ \frac{\partial A_w^{(k+1)}}{\partial A^{(k)}} & \frac{\partial A_w^{(k+1)}}{\partial A_w^{(k)}} & \frac{\partial A_w^{(k+1)}}{\partial A_t^{(k)}} \\ \frac{\partial A_t^{(k+1)}}{\partial A^{(k)}} & \frac{\partial A_t^{(k+1)}}{\partial A_w^{(k)}} & \frac{\partial A_t^{(k+1)}}{\partial A_t^{(k)}} \end{pmatrix} \begin{pmatrix} \frac{\partial A^{(k)}}{\partial x} \\ \frac{\partial A_w^{(k)}}{\partial x} \\ \frac{\partial A_t^{(k)}}{\partial x} \end{pmatrix}, \\ \begin{pmatrix} \frac{\partial A_w^{(k+1)}}{\partial w} \\ \frac{\partial A_t^{(k+1)}}{\partial w} \end{pmatrix} &= \begin{pmatrix} \frac{\partial A_w^{(k+1)}}{\partial A_w^{(k)}} & \frac{\partial A_w^{(k+1)}}{\partial A_t^{(k)}} \\ \frac{\partial A_t^{(k+1)}}{\partial A_w^{(k)}} & \frac{\partial A_t^{(k+1)}}{\partial A_t^{(k)}} \end{pmatrix} \begin{pmatrix} \frac{\partial A_w^{(k)}}{\partial w} \\ \frac{\partial A_t^{(k)}}{\partial w} \end{pmatrix}. \end{aligned} \quad (17)$$

Consequently, starting with the initial conditions (11) and using (4)–(5), (15)–(17), one can analyze the behavior of the average numbers $\langle M \rangle^{(k)}$ and $\langle N \rangle^{(k)}$, when $k \rightarrow \infty$, in the vicinity of each fixed point. Performing such analysis we have found that for $w < w_c(y, t)$ and $x = x_c(y)$, the average number of adsorbed monomers $\langle M \rangle^{(k)}$ quickly approaches some constant value, which indeed is expected for the desorbed phase, whereas $\langle N \rangle^{(k)} \rightarrow \infty$. On the contrary, for both adsorbed phase and the unbinding transition, i.e. when $w \geq w_c(y, t)$, the relation $\langle M \rangle^{(k)} \sim \langle N \rangle^{(k)} \rightarrow \infty$ is satisfied for large k values. This means that limiting value of the fraction of adsorbed monomers of the polymer (which represents the order parameter) changes its value from zero to a non-zero constant at the unbinding transition, implying that this phase transition is of first order. Since $\langle M \rangle^{(k)} / \langle N \rangle^{(k)} \rightarrow \frac{w}{x_c} \left| \frac{dx_c}{dw} \right|$, order of the unbinding transition can also be determined by examination of the first derivative of the critical fugacity x_c behavior in the vicinity of $w = w_c(y, t)$. In Figure 5b we show the dependence of the critical fugacity x_c on the value of w , for $t = 0.6$ and $y = 3.0$. It can be clearly seen that the first derivative of $x_c(y, w, t)$ at $w = w_c(y, t)$ is discontinuous, confirming that the unbinding transition is indeed of first order. Similar plots are obtained for all other values of $t < 1$ and $y > 1$. For $y = 1$, i.e. for the pure adsorption case [21], the line $x_c(y = 1, w, t)$ is smooth, as can be seen in Figure 5a, which means that presence of the force changes the nature of the phase transition under study.

From the definition of Boltzmann factors w and y it follows that temperature and force can be expressed as: $T = |\varepsilon_w| / (k_B \ln w)$, and $f = |\varepsilon_w| \ln y / \ln w$. Thus, knowing $w_c(y, t)$, one can calculate corresponding T and critical

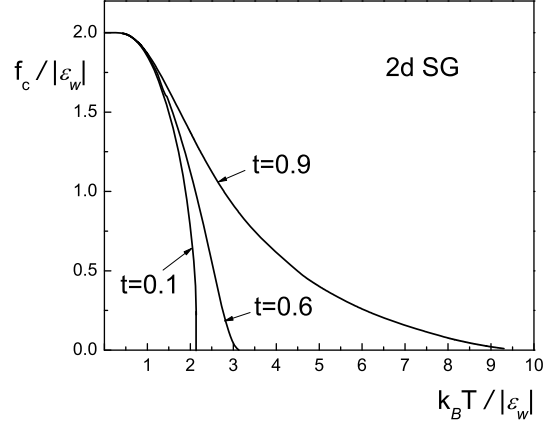


Fig. 6. Force-temperature phase diagram obtained for the 2d Sierpinski gasket case, for $t = 0.1, 0.6, 0.9$.

value $f_c(T)$ of the force, and by varying y , with t fixed, the phase diagram in the (T, f) plane can be obtained. Critical line, plotted for several values of t is shown in Figure 6. One can see that for each value of the surface interaction parameter t the critical force $f_c(T)$ monotonically decreases when T increases, i.e. there is no reentrance. Furthermore, for all t studied we have obtained $f_c / |\varepsilon_w| \rightarrow 2$, when $T \rightarrow 0$, which can be explained in the following way: for low temperatures parameter y is very large and the unbinding fixed point value $F_1^* = 1$ is quickly approached, so that one can take $F_1^{(0)} = x_c(y)y \approx 1$, i.e. $x_c(y) \approx 1/y$ (see Fig. 3). Then, from the initial value $G_2^{(0)} = x_c(y)w_c(t, y)\sqrt{y}$, which should also be close to the corresponding fixed value $G_2^* = 1$, it follows that $w_c(t, y) \approx \sqrt{y}$, and, consequently, $f_c / |\varepsilon_w| \approx 2$. Beyond the low temperature region one can notice that the critical force $f_c(T)$ decreases more rapidly for smaller values of t . This means that at the same temperature weaker force is needed for the desorption of polymer when t is smaller, which certainly could have been expected, since smaller t corresponds to larger repulsion between the surface and the chain segments in the first neighborhood of the wall.

3 Two-dimensional generalization of the Sierpinski gasket case

The framework described in the preceding Section can also be applied on frequently used two-dimensional generalization of the Sierpinski gasket, the so-called Given-Mandelbrot (GM) family of fractals [24]. Each GM fractal is labeled by an integer $b \geq 2$, and it can be constructed starting with a generator that consists of $b(b+1)/2$ unit upward-oriented equilateral triangles, arranged to form a b times larger triangle. Enlarging the generator b times and substituting the smallest triangles with the generator, and then repeating this procedure recursively ad infinitum, one gets a fractal lattice characterized with the integer b . The 2d SG is the first member of this family, with the scaling parameter $b = 2$. Varying b from 2 to ∞ , a whole family of porous lattices, with

fractal dimension $d_f = \ln[b(b+1)/2]/\ln b$, varying from 1.58 to 2, is obtained. Due to their self-similarity, various physical problems on these lattices can be solved exactly, which can be used for systematic examination of how different properties of a physical system depend on its dimensionality. Furthermore, for large b already at the first stage of the construction of the GM fractal, one gets a finite, but large, homogeneous triangular lattice, so that large b extrapolations can be helpful in predicting some results for 2d homogeneous lattices, in cases when other methods are not suitable. Examples of such application of GM fractals are studies of critical behavior of non-interacting SAWs [25–28], and adsorption of SAWs on GM fractals [29–32]. These problems can be scrutinized using restricted partition functions A , A_w , and A_t , defined exactly as in the Sierpinski gasket case. These functions obey recursion relations of the form

$$\begin{aligned} A^{(k+1)} &= \sum_{i=b}^{b(b+1)/2} a_b(i) (A^{(k)})^i, \\ A_w^{(k+1)} &= \alpha_{b,w}(A^{(k)}, A_w^{(k)}, A_t^{(k)}), \\ A_t^{(k+1)} &= \alpha_{b,t}(A^{(k)}, A_w^{(k)}, A_t^{(k)}), \end{aligned} \quad (18)$$

where $a_b(i)$ are positive integers, and functions $\alpha_{b,w}$ and $\alpha_{b,t}$ are polynomials in $A^{(k)}$, $A_w^{(k)}$ and $A_t^{(k)}$. Relations for the bulk function A for b up to 8 can be found in [25], and relations for the surface functions A_w and A_t were obtained in [29] and [30]. Analysis of these relations shows that qualitatively, for $b > 2$ the physical picture remains the same as for $b = 2$, i.e. for each b case considered, there is some critical value of the interaction parameter w , at which transition from adsorbed to desorbed phase occurs. This transition is related to the symmetrical fixed point $(A, A_w, A_t)^* = (A^*, A^*, A^*)$, where A^* is the only non-trivial fixed point of recursion relation for the bulk-function A . The particular values of A^* depend on the scaling parameter value b , but the critical exponents ν and ϕ can be calculated using the same RG framework, as for the 2d Sierpinski gasket. In a similar manner, the force-induced desorption of SAWs on GM fractal with the scaling parameter b can be analyzed generalizing the method applied on the 2d SG case, which we elaborate on in the next paragraph.

Restricted partition functions $F_i^{(k)}(x, y)$, $i = 1, 4$, and $G_i^{(k)}(x, y, w, t)$, $i = 1, 6$, defined as for 2d SG (see Eqs. (7), (8), and Fig. 2), for general b can be expressed via A , A_w , and A_t as

$$\begin{aligned} F_1^{(k)} &= y^{b^k} A^{(k)}, & F_2^{(k)} &= y^{b^k/2} A^{(k)}, \\ F_3^{(k)} &= y^{-b^k/2} A^{(k)}, & F_4^{(k)} &= y^{-b^k} A^{(k)}, \end{aligned} \quad (19)$$

and

$$\begin{aligned} G_1^{(k)} &= y^{b^k} A_t^{(k)}, & G_2^{(k)} &= y^{b^k/2} A_w^{(k)}, \\ G_3^{(k)} &= y^{b^k/2} A_t^{(k)}, & G_4^{(k)} &= y^{-b^k/2} A_w^{(k)}, \\ G_5^{(k)} &= y^{-b^k/2} A_t^{(k)}, & G_6^{(k)} &= y^{-b^k} A_t^{(k)}. \end{aligned} \quad (20)$$

Then, using the grand canonical ensemble formalism, for the SAW average length $\langle N \rangle^{(k)}$ and the average number $\langle M \rangle^{(k)}$ of completely adsorbed SAW steps, one obtains formulae:

$$\langle N \rangle^{(k)} = x \frac{y^{b^k} A_{t,x}^{(k)} + y^{b^k/2} A_{w,x}^{(k)}}{y^{b^k} A_t^{(k)} + y^{b^k/2} A_w^{(k)}}, \quad (21)$$

$$\langle M \rangle^{(k)} = w \frac{y^{b^k} A_{t,w}^{(k)} + y^{b^k/2} A_{w,w}^{(k)}}{y^{b^k} A_t^{(k)} + y^{b^k/2} A_w^{(k)}}, \quad (22)$$

where $A_{t,x} \equiv \frac{\partial A_t}{\partial x}$, $A_{w,x} \equiv \frac{\partial A_w}{\partial x}$, $A_{t,w} \equiv \frac{\partial A_t}{\partial w}$ and $A_{w,w} \equiv \frac{\partial A_w}{\partial w}$. These formulae are straight-forward generalizations of equations (16) and (15), respectively. Therefore, starting with the initial conditions (11), and applying recursion relations for A , A_w , and A_t , obtained in [25] and [29,30], together with the recursion relations for their derivatives, detailed numerical analysis of the problem can be performed. Consequently, for each b considered we obtained results that qualitatively match the $b = 2$ case:

- For each b , $0 < t < 1$, and $y > 1$ there is a critical value $w = w_c(y, t)$ at which unbinding transition happens, so that SAW is adsorbed for $w > w_c$, and desorbed for $w < w_c$.
- The structure of the corresponding fixed points is the same for each b , i.e. $F_2^* = F_3^* = F_4^* = G_3^* = G_4^* = G_5^* = G_6^* = 0$ for all phases, and

$$(F_1, G_1, G_2)^* = \begin{cases} (0, 0, 1), & \text{adsorbed SAW;} \\ (1, G_1^*, 1), & \text{unbinding transition;} \\ (1, G_1^*, 0), & \text{desorbed SAW,} \end{cases} \quad (23)$$

where particular values of $G_1^* > 0$ depend on the values of the interaction parameters, as well as on the value of the scaling parameter b .

- The main difference between the force-induced unbinding transition (when $y > 1$) and the same transition with no acting force (when $y = 1$), is that the former is first order, whereas the latter is second order transition. For the force-induced transition the relation $\langle M \rangle \sim \langle N \rangle$ is valid for each b , whereas for $y = 1$ the relation $\langle M \rangle \sim \langle N \rangle^\phi$ was obtained, with the crossover exponent $\phi \neq 1$, being a non-trivial function of b [29,31].
- The force-temperature phase diagram for $b > 2$ looks qualitatively the same as for $b = 2$ (Fig. 7), i.e. when temperature is decreased, the larger force is required to unbind the SAW. The critical force $f_c(T)$ monotonically increases when T decreases, in such a way that $f_c/|\varepsilon_w| \rightarrow 2$, when $T \rightarrow 0$.

As one can see in Figure 7, for larger temperatures the curve $f_c(T)$ becomes steeper as b grows (for the same t value). This means that weaker force is required for unbinding the chain from the wall when b is larger, so one might expect that the value of the critical force for regular triangular lattice is smaller than the corresponding one for

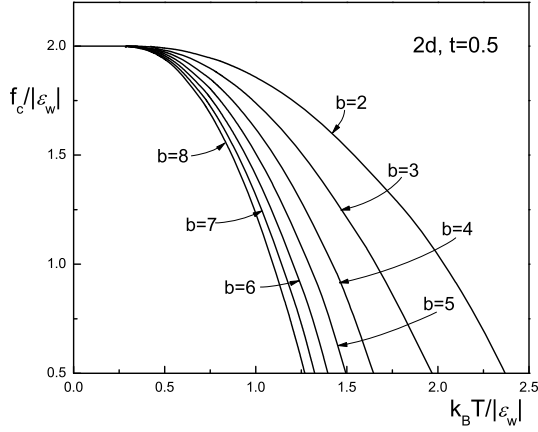


Fig. 7. Force-temperature phase diagram obtained for the Given-Mandelbrot fractals for $t = 0.5$ and $2 \leq b \leq 8$.

any of GM fractal lattices. One can also notice that differences between the $f_c(T)$ curves become smaller as b grows and it seems that in the limit $b \rightarrow \infty$ they could collapse on one curve, which might correspond to the triangular lattice.

4 The three-dimensional generalization

In this Section we study the force-induced desorption of SAW on fractals that belong to a family which represents a three-dimensional generalization of the Sierpinski gasket fractal. The 3d SG fractal can be constructed recursively as GM fractal, with the only difference that the generator of the fractal with the parameter b is no longer a triangle, but a tetrahedron that contains $b(b+1)(b+2)/6$ smaller upward-oriented tetrahedrons.

As it was elaborated in [22,23,33–35], SAWs on 3d SG fractals can be analyzed within the exact real-space RG approach, similar to that applied in the case of GM fractals. The main difference between these two cases is that in the 3d SG fractal case one needs additional restricted partition function, $B^{(k)}(x)$, which represents the second RG parameter, and corresponds to two-stranded SAW configurations (see Fig. 8a) on the k th order gasket (which cannot exist on GM fractals due to their topology). In particular, the function $B^{(k)}(x)$ is defined as

$$B^{(k)}(x) = \sum_N \mathcal{B}^{(k)}(N) x^N,$$

where $\mathcal{B}^{(k)}(N)$ is the number of N -step SAW configurations, which consist of two mutually avoiding self-avoiding walks traversing the k th order gasket. Functions $A^{(k)}(x)$ (defined in the same way as in the 2d case) and $B^{(k)}(x)$ fulfil a closed set of recursion relations

$$\begin{aligned} A^{(k+1)} &= \alpha_b(A^{(k)}, B^{(k)}), \\ B^{(k+1)} &= \beta_b(A^{(k)}, B^{(k)}), \end{aligned} \quad (24)$$

where functions α_b and β_b are polynomials, whose particular form depends only on the value of the fractal scaling

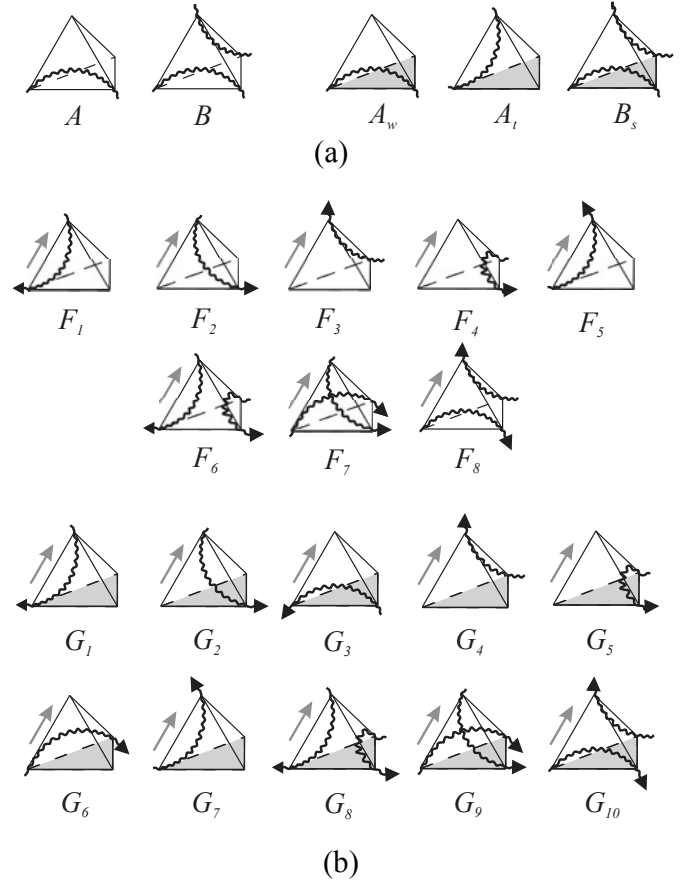


Fig. 8. Schematic presentation of the SAW configurations corresponding to all restricted partition functions needed for analysis of the force-induced desorption on 3d Sierpinski gaskets. Tetrahedrons represent k th order gaskets, straight gray arrows denote the direction of the force, gray faces correspond to the adsorbing wall, whereas wavy lines are parts of the SAW. When force is not present, one-stranded F_i -type configurations ($i = 1, \dots, 5$), spanning through gaskets which are completely in the bulk of the fractal structure, become identical to A -type SAW configurations, whereas two-stranded F_6, F_7 and F_8 reduce to B -type configurations. In a similar way, G_i -type configurations within gaskets which lie on the adsorbing wall, reduce to A_w, A_t or B_s , when $f = 0$.

parameter b . Analysis of the exact RG relations (24) for b up to 4 showed that, within the model of non-interacting SAW, only one non-trivial fixed point (A^*, B^*) can be reached, and it corresponds to the swollen isotropic coil in the bulk [22,33–35].

Assuming that one of the boundary faces of 3d SG fractal is an adsorbing wall, SAW adsorption can be studied [21,35] using exact real-space RG scheme, in which in addition to bulk-functions $A^{(k)}(x)$ and $B^{(k)}(x)$, surface-functions $A_w^{(k)}(x, w, t)$, $A_t^{(k)}(x, w, t)$ and $B_s^{(k)}(x, w, t)$ are introduced (Fig. 8). Whereas $A_w^{(k)}$ and $A_t^{(k)}$ are defined as in the 2d case, function $B_s^{(k)}$ is equal to

$$B_s^{(k)}(x, w, t) = \sum_{N, M, R} \mathcal{B}_s^{(k)}(N, M, R) x^N w^M t^R,$$

where $B_s^{(k)}(N, M, R)$ is the number of N -step two-stranded SAW configurations, with M steps at the adsorbing wall and R steps in the layer adjacent to the wall. For each b , functions $A_w^{(k)}$, $A_t^{(k)}$ and $B_s^{(k)}$ obey recursion relations of the form

$$\begin{aligned} A_w^{(k+1)} &= \alpha_{b,w}(A^{(k)}, B^{(k)}, A_w^{(k)}, A_t^{(k)}, B_s^{(k)}), \\ A_t^{(k+1)} &= \alpha_{b,t}(A^{(k)}, B^{(k)}, A_w^{(k)}, A_t^{(k)}, B_s^{(k)}), \\ B_s^{(k+1)} &= \beta_{b,s}(A^{(k)}, B^{(k)}, A_w^{(k)}, A_t^{(k)}, B_s^{(k)}), \end{aligned} \quad (25)$$

where $\alpha_{b,w}$, $\alpha_{b,t}$ and $\beta_{b,s}$ are polynomials in $A^{(k)}$, $B^{(k)}$, $A_w^{(k)}$, $A_t^{(k)}$ and $B_s^{(k)}$. Numerical examination of the exact RG equations (24) and (25), performed in [21] for $b = 2$, and in [35] for $b = 3$ and 4, revealed that for each $0 < t < 1$ an unbinding transition occurs at some critical value $w = w^*(t)$. For this value of w and $x = x^*$, where x^* is the bulk critical fugacity for which values of the bulk functions $(A^{(k)}, B^{(k)})$ tend to the SAW fixed point (A^*, B^*) , and the surface functions $(A_w^{(k)}, A_t^{(k)}, B_s^{(k)})$ tend to (A^*, A^*, B^*) , when $k \rightarrow \infty$. At this fixed point, average number $\langle M \rangle$ of adsorbed SAW steps scales as $\langle M \rangle \sim \langle N \rangle^\phi$ with the average SAW length $\langle N \rangle$. Using the exact RG transformations, the values $\phi = 0.7481$, 0.7162 and 0.6907 were obtained for $b = 2, 3$ and 4, respectively, whereas for b up to 40, crossover exponent was calculated using the Monte Carlo RG approach [35].

For weaker surface attraction, i.e. when $w < w^*(t)$, polymer is desorbed and the corresponding fixed point

$$(A, B, A_w, A_t, B_s)^* = (A^*, B^*, 0, 0, 0)$$

is reached for $x = x^*$. For $w > w^*(t)$, finite fixed values of surface-functions can be obtained only by lowering the fugacity, so that for $x = x_c(w, t) < x^*$, the fixed point

$$(A, B, A_w, A_t, B_s)^* = (0, 0, A_{2d}^*, 0, 0)$$

is obtained. The value A_{2d}^* is equal to the bulk fixed point for SAW on the corresponding GM fractal, which is in accord with the fact that in this case polymer is completely adsorbed at the boundary wall (itself being a GM fractal).

4.1 Force-induced desorption of SAW on 3d SG fractals

To study the influence of the stretching force, acting along an edge of the 3d SG which is not in the adsorbing boundary, on the behavior of SAW, we introduce 18 restricted partition functions:

$$F_i^{(k)}(x, y) = \sum_{N, L} \mathcal{F}_i^{(k)}(N, L) x^N y^L, \quad i = 1, 8 \quad (26)$$

$$\begin{aligned} G_i^{(k)}(x, y, w, t) &= \sum_{N, M, R, L} \mathcal{G}_i^{(k)}(N, M, R, L) x^N w^M t^R y^L, \\ i &= 1, 10 \end{aligned} \quad (27)$$

where parameters x, y, w and t are defined in the same way as for the GM fractals, $\mathcal{F}_i^{(k)}(N, L)$ are the numbers of SAW configurations which span the k th order gaskets that are entirely in the bulk of the fractal, whereas numbers $\mathcal{G}_i^{(k)}(N, M, R, L)$ correspond to configurations within the k th order gaskets lying in the surface. Numbers \mathcal{F}_i , for $i = 1, \dots, 5$, and \mathcal{G}_i , for $i = 1, \dots, 7$ correspond to single-stranded configurations, whereas all the remaining \mathcal{F}_i and \mathcal{G}_i enumerate double-stranded configurations, as depicted in Figure 8b. Knowing $A^{(k)}$, $B^{(k)}$, $A_w^{(k)}$, $A_t^{(k)}$ and $B_s^{(k)}$, one can find $F_i^{(k)}$ and $G_i^{(k)}$ using formulae:

$$\begin{aligned} F_1^{(k)} &= y^{-b^k} A^{(k)}, & F_2^{(k)} &= y^{-b^k/2} A^{(k)}, \\ F_3^{(k)} &= y^{b^k/2} A^{(k)}, & F_4^{(k)} &= A^{(k)}, \\ F_5^{(k)} &= y^{b^k} A^{(k)}, & F_6^{(k)} &= y^{-b^k} B^{(k)}, \\ F_7^{(k)} &= B^{(k)}, & F_8^{(k)} &= y^{b^k} B^{(k)}, \\ G_1^{(k)} &= y^{-b^k} A_t^{(k)}, & G_2^{(k)} &= y^{-b^k/2} A_t^{(k)}, \\ G_3^{(k)} &= y^{-b^k/2} A_w^{(k)}, & G_4^{(k)} &= y^{b^k/2} A_t^{(k)}, \\ G_5^{(k)} &= A_w^{(k)}, & G_6^{(k)} &= y^{b^k/2} A_w^{(k)}, \\ G_7^{(k)} &= y^{b^k} A_t^{(k)}, & G_8^{(k)} &= y^{-b^k} B_s^{(k)}, \\ G_9^{(k)} &= B_s^{(k)}, & G_{10}^{(k)} &= y^{b^k} B_s^{(k)}. \end{aligned} \quad (28)$$

Then, performing a similar, but technically more complicated analysis than in the 2d case (see Appendix B for some details), we have found that for $b = 2, 3$ and 4, there are three physically relevant fixed points, corresponding to unbinding transition, adsorbed and desorbed polymer phase:

1. The fixed point

$$F_{1,2,3,4,6,7,8}^* = G_{1,2,3,4,5,6,8,9,10}^* = 0, \quad F_5^* = 1, \quad G_7^* > 0$$

corresponds to the **desorbed phase**. This point is obtained for weak surface attraction $1 < w < w_c(y, t)$. In this phase SAW is elongated along the direction of the force. The critical fugacity for this phase is equal to $x = x_c(y) < x_c(y = 1) = x^*$, and depends only on the value of y . The value of $G_7^* > 0$ is finite and depends on the particular values of t and w (and b). The fraction of adsorbed monomers $\langle M \rangle^{(k)} / \langle N \rangle^{(k)} \rightarrow 0$, as $k \rightarrow \infty$.

2. For strong surface attraction, when $w > w_c(y, t)$, the fixed point

$$F_i^* = 0, \quad G_{1,2,3,4,5,7,8,9,10}^* = 0, \quad G_6^* = 1,$$

corresponding to the **adsorbed phase**, can be reached starting with the critical fugacity $x = x_c(y, t, w)$. This fugacity is smaller than the value $x_c(y)$ obtained for the desorbed phase for the same value of y and t , and monotonically decreases with w . The fraction of monomers adsorbed at the wall tends to a non-zero constant value as $k \rightarrow \infty$.

3. For the critical value of the surface attraction $w = w_c(y, t)$, and the critical fugacity $x_c(y)$, found for the

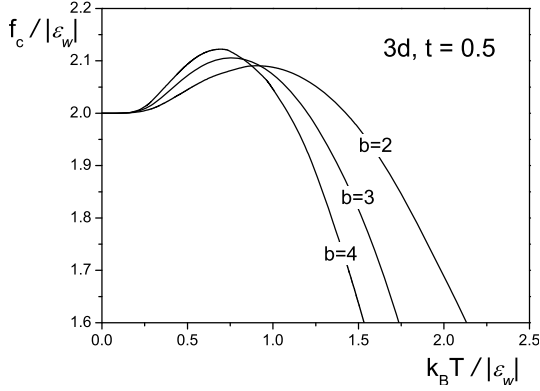


Fig. 9. Force-temperature phase diagram obtained for the 3d Sierpinski gasket fractals with $b = 2, 3$ and 4 , for $t = 0.5$.

desorbed phase, the fixed point

$$F_{1,2,3,4,6,7,8}^* = G_{1,2,3,4,5,8,9,10}^* = 0,$$

$$F_5^* = 1, G_6^* = 1, G_7^* > 0$$

is obtained. It corresponds to the **unbinding transition**. The SAW is elongated, but large number of its steps are adsorbed, so that, as for the adsorbed phase, relation $\langle M \rangle^{(k)} \sim \langle N \rangle^{(k)}$ is valid for $k \rightarrow \infty$.

The unbinding transition is of first order, and dependence of critical fugacity x_c on the surface attraction strength w (when t and y are fixed) is qualitatively the same as for GM fractals (Fig. 5b), with the first derivative being discontinuous at the critical value $w = w_c$.

So far, the obtained physical pictures of the force-induced desorption of SAW on 2d and 3d fractals appear to be the same, but this changes when one looks at the 3d force-temperature phase diagram in Figure 9. In contrast to the diagram obtained for GM fractals (Fig. 7), this diagram is reentrant for each studied b . The similar reentrant diagrams were also obtained for large number of other t values between 0 and 1. The critical force at which SAW desorbs from the wall at low temperatures grows with T , until it reaches its maximum at some finite value of T , and then it monotonically decreases as T becomes larger. As for the $T \rightarrow 0$ limit, following the same line of reasoning as in the 2d case, it can be shown that $f_c/|\varepsilon_w| \rightarrow 2$. Finally, one can notice that the maximum value of the critical force becomes larger as b grows, whereas the temperature at which this maximum occurs decreases. This could mean that larger degree of inhomogeneity (measured by deviation of fractal dimension, $\ln[b(b+1)(b+2)]/\ln b$ for 3d SG, from dimension $d = 3$ of embedding space) makes the reentrance less pronounced, however such a conclusion needs additional investigation, which is beyond the scope of this paper.

5 Summary and conclusions

In this paper we have studied the force-induced desorption of a linear polymer chain in a good solvent, modeled by a

self-avoiding walk on Sierpinski gasket lattice and its two- and three-dimensional generalizations: Given-Mandelbrot and 3d SG fractals. In all studied cases SAW interacts with the adsorbing wall, represented by one of the lattice boundaries, and it is pulled away from the wall by an external force f , directed along an edge not lying in the wall. By applying an exact real-space renormalization group approach, which can also be interpreted as a grand canonical ensemble formalism, we have performed detailed numerical analysis of the phase diagram, for various values of the interaction parameters. For all studied lattices we have found that when $f > 0$ the unbinding transition is of first order, meaning that the presence of pulling force changes the nature of the corresponding transition driven only by temperature. This is in accord with the results obtained for the force-induced desorption of SAWs on homogeneous lattices, using Monte Carlo [8] and exact enumeration [10] techniques, as well as with the analytically obtained results for directed SAW models [7,11,12,16,18,19].

The unbinding transition from adsorbed to desorbed phase occurs at some critical value of the force $f_c(T)$, which is presented in Figures 6, 7 and 9 for some cases studied here. One can observe the apparent qualitative difference between the diagrams obtained for lattices embedded in 2d and 3d space: whereas in all 2d cases $f_c(T)$ is a monotonically decreasing function of T , being almost constant in the region of very low temperatures (Fig. 6 and Fig. 7), in all 3d cases $f_c(T)$ increases in the low-temperature region, goes through a maximum as T varies, and decreases in the high-temperature region (Fig. 9). Decreasing of the critical force with T is intuitively acceptable, since higher temperatures favour desorption, therefore weaker force is needed to detach polymer from the wall, and monotonically decreasing $f_c(T)$ were indeed found in the previous studies of force-induced desorption on square lattice. However, reentrant $f_c(T)$ diagrams were established for all previously studied 3d models on homogeneous lattices. It was elaborated in [7,10] that low-temperature behavior of the critical force diagram is governed by the competition between the number of possible conformations corresponding to the desorbed and adsorbed polymers. Whereas desorbed polymer can be in only one conformation at zero temperature, i.e. elongated along the direction of the force, the number of adsorbed conformations is much larger for all studied SAW models, except in 2d cases, where adsorbed polymer can only be elongated along the adsorbing wall, which is a line. This seems to be the reason why in the low-temperature region the critical force is almost constant in 2d cases, while in 3d cases it increases. In the case of GM fractals adsorbing wall is also a line, whereas in the 3d case adsorbing wall is corresponding GM fractal, for which large number of polymer conformations is possible. In that sense, fractal cases studied here do not differ significantly from the previously studied homogeneous cases and we can say that our results support such explanation of the reentrant critical force diagram.

Comparing the phase diagrams obtained for different 2d fractals (Fig. 7) one can notice that as fractal scaling

parameter b grows the difference between the corresponding diagrams becomes smaller. Therefore, one might accept results obtained for GM fractals as approximate results for the triangular lattice, for which the force-induced desorption has not been studied so far. In that sense, it would be desirable to investigate larger b cases, possibly with some other method, such as finite-size scaling, which proved to be useful in analysis of the critical SAW behavior at the fractal-to-Euclidean lattice crossover region $b \rightarrow \infty$ [26,27,29]. Also, having in mind the accomplishments of directed models studies [7,9,11,12,16–19] it would be interesting to extend the corresponding piece-wise directed walk model on GM fractals [36,37] in such a way that it can be used for analysis of the force-induced desorption.

Finally, we should mention that from the point of view of possible applications, 3d SG fractals are much more interesting than GM fractals. Due to their complex topology fewer results can be obtained for them, but the range of physical phenomena that can be investigated is much broader comparing to 2d cases. For instance, introducing self-attraction into the self-avoiding walk model gives rise to the occurrence of the collapse transition from swollen to compact phase on 3d SG, but not on GM fractals [33–35]. Therefore, in the future we also intend to enrich the 3d SG model studied here by adding other interactions in order to obtain more realistic picture of the related phenomena.

This paper has been produced as a part of the work within the project No. 171015, funded by the Serbian Ministry of Science and Technological Development. We are grateful to I. Živić for careful and critical reading of the manuscript.

Appendix A: Large k behavior of the partition functions $F_i^{(k)}$ and $G_i^{(k)}$ for the 2d Sierpinski gasket lattice

In this appendix we give some details of the analysis of the large k behavior of the restricted partition functions $F_i^{(k)}(x, y)$ and $G_i^{(k)}(x, y, w, t)$, performed in the case of Sierpinski gasket lattice in order to find polymer phases, described in Section 2.

From relations (9), for the force-functions, it follows that for $x = x^*$ and $y > 1$ functions $F_1^{(k)}(x, y)$ and $F_2^{(k)}(x, y)$ tend to ∞ when $k \rightarrow \infty$, since $A^{(k)}(x^*) = A^* = (\sqrt{5} - 1)/2$. Therefore, in order to obtain finite values for $F_1^{(k)}$ and $F_2^{(k)}$, one should take $x < x^*$. On the other hand, for $x < x^*$ function $A^{(k)}(x)$ quickly approaches 0, which means that relation (4) can be approximated with the relation

$$A^{(k+1)} \approx (A^{(k)})^2,$$

implying that for $k \gg 1$, $A^{(k)}(x)$ behaves as λ^{2k} , with $\lambda = \lambda(x) < 1$. Then, from (9) it follows that for $x < x^*$

and $k \gg 1$ relations

$$F_1^{(k)} \sim (\lambda y)^{2k}, \quad F_2^{(k)} \sim (\lambda \sqrt{y})^{2k}, \\ F_3^{(k)} \sim \left(\frac{\lambda}{\sqrt{y}}\right)^{2k}, \quad F_4^{(k)} \sim \left(\frac{\lambda}{y}\right)^{2k}$$

are valid. This means that for $x < x^*$ and $y \neq 1/\lambda$, function $F_1^{(k)}(x, y)$ becomes either infinitely large or tends to 0, when $k \rightarrow \infty$. Since for $y > 1$ inequality $F_1 > F_2, F_3, F_4$ is always satisfied, it follows that nontrivial finite fixed point $(F_1, F_2, F_3, F_4)^*$ can be expected only for $y = 1/\lambda$. Numerical analysis of equations (4) and (9) certainly confirms this expectation, i.e. for all $x < x^*$ studied, already for small values of k , function $\ln A^{(k)}(x)/2^k$ reaches a constant value $\ln \lambda$, which does not alter significantly when k grows, and then, taking $y = 1/\lambda$, one obtains

$$(F_1, F_2, F_3, F_4)^{(k)} \rightarrow (F_1, F_2, F_3, F_4)^* = (1, 0, 0, 0).$$

In this way a line $x = x_c(y)$ (see Fig. 3) is found, so that one can conclude that for each $y > 1$ there is a critical value $x_c(y) < x^*$, such that for $x = x_c(y)$ the fixed point $(F_1^* = 1, 0, 0, 0)$ is obtained. Since for $y = 1$ all $F_i^{(k)}$ are identically equal to $A^{(k)}$, and for $x = x^*$ the RG fixed point A^* of the pure SAW model is recovered, one observes that presence of even extremely weak force breaks the isotropy of the coil, which corresponds to the fact that SAW is always elongated by the force.

From equations (10) for the force-surface-functions $G_i^{(k)}$ it follows that in the limit $k \rightarrow \infty$ functions G_1 , G_2 and G_3 become infinitely large, unless $A_w^{(k)}, A_t^{(k)} \rightarrow 0$. Numerically analyzing recursion relations (5) for surface-functions A_w and A_t , simultaneously with the relation (4) for the bulk-function A , one can find that for $x < x^*$, $w > 1$ and $0 < t < 1$, functions A_w and A_t behave as

$$A_w^{(k)} \sim \lambda_w^{2k}, \quad A_t^{(k)} \sim \lambda_t^{2k},$$

when $k \rightarrow \infty$ (where values of λ_w and λ_t depend on x , w and t), which implies that

$$G_1^{(k)} \sim (y\lambda_t)^{2k}, \quad G_2^{(k)} \sim (\sqrt{y}\lambda_w)^{2k}.$$

The condition $x < x^*$ is required to maintain $F_1^{(k)}$ finite, and since in that case $A^{(k)} \sim \lambda^{2k}$, one can expect the following physically relevant situations:

1. $1/y = \lambda = \lambda_t = \lambda_w^2$, in which case $F_1^{(k)} \rightarrow 1$, $G_1^{(k)} \rightarrow \text{const.} > 0$, $G_2^{(k)} \rightarrow \text{const.} > 0$.
2. $1/y = \lambda = \lambda_t > \lambda_w^2$, corresponding to $F_1^{(k)} \rightarrow 1$, $G_1^{(k)} \rightarrow \text{const.} > 0$, $G_2^{(k)} \rightarrow 0$.
3. $1/y = \lambda_w^2 > \max(\lambda_t, \lambda)$, when $F_1^{(k)}, G_1^{(k)} \rightarrow 0$, and $G_2^{(k)} \rightarrow \text{const.} > 0$.

Detailed numerical analysis confirmed that:

1. $\lambda = \lambda_t = \lambda_w^2$ is obtained for every $y > 1$ and $0 < t < 1$, if $x = x_c(y)$ and $w = w_c(y, t)$ (Fig. 4), which corresponds to the fixed point (12).

2. For $w < w_c(y, t)$, $x = x_c(y)$, $y > 1$ and $0 < t < 1$ one obtains $1/y = \lambda = \lambda_t > \lambda_w^2$, and the corresponding fixed point is (13).
3. When $w > w_c(y, t)$, and $x = x_c(y)$, for any $y > 1$ and $0 < t < 1$, the value of $G_2^{(k)}$ becomes infinitely large as k increases. Therefore, one should decrease x , until finite limiting value for G_2 is obtained. Eventually, this happens for some value $x = x_c(w, y, t) < x_c(y)$ (see Fig. 5), in which case $1/y = \lambda_w^2 > \max(\lambda_t, \lambda)$, and the corresponding fixed point is (14).

Appendix B: Details of the analysis of the 3d case

The physically relevant fixed points in the 3d case, described in Section 4, were found by using the relations (28) and (29), together with the recursion relations (25) for the functions A_t , A_w , and B_s , and relations (24) for the functions A , B , starting with the initial values

$$\begin{aligned} A^{(0)} &= x, & A_t^{(0)} &= xt, & A_w^{(0)} &= xw, \\ B^{(0)} &= x^2, & B_s^{(0)} &= x^2wt. \end{aligned}$$

This was performed for $b = 2, 3$ and 4 , for which relations (24) and (25) were established previously [21,22,33,35].

Analysis of the behavior of the order parameter $\langle M \rangle / \langle N \rangle$ has been done by taking $(2G_6^{(k)} + G_7^{(k)})$ as the grand canonical partition function for SAWs with the first point at a fixed corner of the k th order gasket lying on the surface. In that approach, using relations (29), the average length $\langle N \rangle^{(k)}$ and the average number of adsorbed monomers $\langle M \rangle^{(k)}$ can be put in the following forms:

$$\begin{aligned} \langle N \rangle^{(k)} &= x \frac{y^{b^k} A_{t,x}^{(k)} + 2y^{b^k/2} A_{w,x}^{(k)}}{y^{b^k} A_t^{(k)} + 2y^{b^k/2} A_w^{(k)}}, \\ \langle M \rangle^{(k)} &= w \frac{y^{b^k} A_{t,w}^{(k)} + 2y^{b^k/2} A_{w,w}^{(k)}}{y^{b^k} A_t^{(k)} + 2y^{b^k/2} A_w^{(k)}}. \end{aligned}$$

Then, again using recursion relations for the functions A_t , A_w , B_s , A , and B , together with the relations for the derivatives:

$$\begin{aligned} \begin{pmatrix} \frac{\partial A^{(k+1)}}{\partial x} \\ \frac{\partial B^{(k+1)}}{\partial x} \\ \frac{\partial A_w^{(k+1)}}{\partial x} \\ \frac{\partial A_t^{(k+1)}}{\partial x} \\ \frac{\partial B_s^{(k+1)}}{\partial x} \end{pmatrix} &= \mathbf{R} \begin{pmatrix} \frac{\partial A^{(k)}}{\partial x} \\ \frac{\partial B^{(k)}}{\partial x} \\ \frac{\partial A_w^{(k)}}{\partial x} \\ \frac{\partial A_t^{(k)}}{\partial x} \\ \frac{\partial B_s^{(k)}}{\partial x} \end{pmatrix}, \\ \begin{pmatrix} \frac{\partial A^{(k+1)}}{\partial w} \\ \frac{\partial A_t^{(k+1)}}{\partial w} \\ \frac{\partial B_s^{(k+1)}}{\partial w} \end{pmatrix} &= \mathbf{R}_S \begin{pmatrix} \frac{\partial A^{(k)}}{\partial w} \\ \frac{\partial A_t^{(k)}}{\partial w} \\ \frac{\partial B_s^{(k)}}{\partial w} \end{pmatrix} \end{aligned}$$

where matrices \mathbf{R} and \mathbf{R}_S are equal to

$$\mathbf{R} = \begin{pmatrix} \frac{\partial A^{(k+1)}}{\partial A^{(k)}} & \frac{\partial A^{(k+1)}}{\partial B^{(k)}} & 0 & 0 & 0 \\ \frac{\partial B^{(k+1)}}{\partial A^{(k)}} & \frac{\partial B^{(k+1)}}{\partial B^{(k)}} & 0 & 0 & 0 \\ \frac{\partial A_w^{(k+1)}}{\partial A^{(k)}} & \frac{\partial A_w^{(k+1)}}{\partial B^{(k)}} & \frac{\partial A_w^{(k+1)}}{\partial A_w^{(k)}} & \frac{\partial A_w^{(k+1)}}{\partial A_t^{(k)}} & \frac{\partial A_w^{(k+1)}}{\partial B_s^{(k)}} \\ \frac{\partial A_t^{(k+1)}}{\partial A^{(k)}} & \frac{\partial A_t^{(k+1)}}{\partial B^{(k)}} & \frac{\partial A_t^{(k+1)}}{\partial A_w^{(k)}} & \frac{\partial A_t^{(k+1)}}{\partial A_t^{(k)}} & \frac{\partial A_t^{(k+1)}}{\partial B_s^{(k)}} \\ \frac{\partial B_s^{(k+1)}}{\partial A^{(k)}} & \frac{\partial B_s^{(k+1)}}{\partial B^{(k)}} & \frac{\partial B_s^{(k+1)}}{\partial A_w^{(k)}} & \frac{\partial B_s^{(k+1)}}{\partial A_t^{(k)}} & \frac{\partial B_s^{(k+1)}}{\partial B_s^{(k)}} \end{pmatrix},$$

and

$$\mathbf{R}_S = \begin{pmatrix} \frac{\partial A_w^{(k+1)}}{\partial A_w^{(k)}} & \frac{\partial A_w^{(k+1)}}{\partial A_t^{(k)}} & \frac{\partial A_w^{(k+1)}}{\partial B_s^{(k)}} \\ \frac{\partial A_t^{(k+1)}}{\partial A_w^{(k)}} & \frac{\partial A_t^{(k+1)}}{\partial A_t^{(k)}} & \frac{\partial A_t^{(k+1)}}{\partial B_s^{(k)}} \\ \frac{\partial B_s^{(k+1)}}{\partial A_w^{(k)}} & \frac{\partial B_s^{(k+1)}}{\partial A_t^{(k)}} & \frac{\partial B_s^{(k+1)}}{\partial B_s^{(k)}} \end{pmatrix}$$

we have examined behavior of $\langle M \rangle^{(k)} / \langle N \rangle^{(k)}$ for large number of $y > 1$, $w > 1$ and $0 < t < 1$ values, and corresponding critical values of x , for $k \gg 1$, in the cases of $b = 2, 3$, and 4 .

References

1. F. Ritort, J. Phys.: Condens. Matter **18**, R531 (2006)
2. P.G. de Gennes, *Scaling Concepts in Polymer Physics* (Cornell University Press, Ithaca, 1979)
3. K. Dé Bell, T. Lookman, Rev. Mod. Phys. **65**, 87 (1993)
4. C. Vanderzande, *Lattice Models of Polymers* (Cambridge University Press, Cambridge, 1998)
5. B. Haupt, J. Ennis, M. Sevick, Langmuir **15**, 3886 (1999)
6. A.M. Skvortsov, L.I. Klushin, T.M. Birshtein, Polymer. Sci. (Russia) Ser. A **51**, 469 (2009)
7. E. Orlandini, M.C. Tesi, S.G. Whittington, J. Phys. A: Math. Gen. **37**, 1535 (2004)
8. J. Krawczyk, T. Prellberg, A.L. Owczarek, A. Rechnitzer, J. Stat. Mech.: Theor. Exp. P10004 (2004)
9. G. Iliev, E. Orlandini, S.G. Whittington, Eur. Phys. J. B **40**, 63 (2004)
10. P.K. Mishra, S. Kumar, Y. Singh, Europhys. Lett. **69**, 102 (2005)
11. E. Orlandini, M.C. Tesi, J. Math. Chem. **45**, 72 (2009)
12. P.-M. Lam, Y. Zhen, H. Zhou, J. Zhou, Phys. Rev. E **79**, 061127 (2009)
13. S. Bhattacharya, A. Milchev, V.G. Rostiashvili, T.A. Vilgis, Eur. Phys. J. E **29**, 285 (2009)
14. S. Bhattacharya, V.G. Rostiashvili, A. Milchev, T.A. Vilgis, Phys. Rev. E **79**, R030802 (2009)
15. S. Bhattacharya, V.G. Rostiashvili, A. Milchev, T.A. Vilgis, Macromolecules **42**, 2236 (2009)
16. J. Alvarez, S.G. Whittington, J. Stat. Mech.: Theor. Exp. P04016 (2009)
17. A.L. Owczarek, J. Phys. A: Math. Theor. **43**, 225002 (2010)
18. G.K. Iliev, E. Orlandini, S.G. Whittington, J. Phys. A: Math. Theor. **43**, 315202 (2010)

19. J. Osborn, T. Prellberg, *J. Stat. Mech.: Theor. Exp.* P09018 (2010)
20. D. Dhar, Y. Singh, *Linear and Branched Polymers on Fractals*, a chapter in *Statistics of Linear Polymers in Disordered Media*, edited by B.K. Chakrabarti (Elsevier, Amsterdam, 2005)
21. E. Bouchaud, J. Vannimenus, *J. Phys. (Paris)* **50**, 2931 (1989)
22. D. Dhar, *J. Math. Phys.* **19**, 5 (1978)
23. R. Rammal, G. Toulouse, J. Vannimenus, *J. Phys. (Paris)* **45**, 389 (1984)
24. J.A. Given, B.B. Mandelbrot, *J. Phys. A* **16**, L565 (1983)
25. S. Elezović, M. Knežević, S. Milošević, *J. Phys. A* **20**, 1215 (1987)
26. D. Dhar, *J. Phys. France* **49**, 397 (1988)
27. S. Milošević, I. Živić, *J. Phys. A: Math. Gen.* **24**, L833 (1991)
28. F.A.C.C. Chalub, F.D.D.A. Reis, R. Riera, *J. Phys. A: Math. Gen.* **30**, 4151 (1997)
29. S. Kumar, Y. Singh, D. Dhar, *J. Phys. A: Math. Gen.* **26**, 4835 (1993)
30. V. Bubanja, M. Knežević, J. Vannimenus, *J. Stat. Phys.* **71**, 1 (1993)
31. I. Živić, S. Milošević, E.H. Stanley, *Phys. Rev. E* **49**, 636 (1994)
32. S. Elezović-Hadžić, M. Knežević, S. Milošević, I. Živić, *J. Stat. Phys.* **83**, 1241 (1996)
33. D. Dhar, J. Vannimenus, *J. Phys. A: Math. Gen.* **20**, 199 (1987)
34. M. Knežević, J. Vannimenus, *J. Phys. A: Math. Gen.* **20**, L969 (1987)
35. S. Elezović-Hadžić, I. Živić, S. Milošević, *J. Phys. A: Math. Gen.* **36**, 1213 (2003)
36. S. Elezović-Hadžić, S. Milošević, H.W. Capel, G.L. Wiersma, *Physica A* **150**, 402 (1988)
37. S. Elezović-Hadžić, N. Vasiljević, *J. Phys. A: Math. Gen.* **32**, 1329 (1999)